TEMPERATURE DEPENDENCE OF DYNAMIC FRACTURE TOUGHNESS OF TWO STEELS UNDER STRESS PULSE LOADING

H. HOMMA*, N. WATANABE**, and H. NAKAZAWA***

A new test device was constructed to measure dynamic fracture toughness under stress wave loading. Using the test device, temperature dependence of the dynamic fracture toughness of two structural steels, ASTM A533B steel and JIS SK4 steel, under $\dot{K}$ of about 1×10^6 MPa$\sqrt{m}$ /s was investigated in the range of 20 to -100 C. The temperature dependence for the two stells was much moderate in comparison with that of the quasi-static fracture toughness.
This is interpreted by no change of the microscopic fracture mechanism. Measured stretched zone width also corresponds to the temperature dependence of the dynamic fracture toughness for the two steels.

INTRODUCTION

Fracture toughness under a quasi-static high loading rate can be definitely measured by a method based on the standard of plane strain fracture toughness testing method for metallic materials(1) established by the American Society for Testing and Materials(ASTM), if response of an used measuring system is quick enough. Also, for impact loading, instrumented Charpy impact test or dynamic tear test has been used to evaluate the dynamic fracture toughness(2). However, there are two problems in such test methods: the one is the limitation of impact velocity up to the value where stress field in a specimen would be dominated by dynamic effect, in other words, inertia effect; the other is the uncertain determination of crack initiation load.

The former results from the fact that the knowledge of dynamic stress intensity factors for different specimen geometries under various load histories is lack. This can be resolved if the full dynamic stress analysis is done for the used specimen on the aid of finite element code or finite difference code.

The latter results from the difficulty in detection of crack initiation. Usually, the maximum load in the impact load history is conveniently defined as the crack initiation load.

In fully dynamic tear test, Kalthoff et al(3) used the shadow optical method near a crack tip to detect the crack initiation.

Costin et al(4) determined the crack initiation load from the load-displacement curve in accordance with the ASTM standards E399 by usuing the 5 percent slope offset procedure in the dynamic fracture split-Hopinson bar test apparatus. They used the Moire fringe technique to measure the crack opening displacement.

* Dept. Energy Engineering, Toyohashi University of Technology, 1-1 Tempaku-cho, Toyohashi 440, Japan
** Canon Co. Ltd. 2-7-1 Nishi-shinjuku, Shinjuku-ku,Tokyo 160, Japan
*** Dept. Physical Engineering, Tokyo Institute of Technology, 2-12-1 Ohokayama, Meguro-ku, Tokyo 152, Japan

Some workers(5,6) used the strain gage output mounted near the crack tip. Sensitivity of the detection would much depend on the distance of the strain gage to the crack tip and affected by the crack tip plasticity.

In this paper, the test method proposed by the present author(7) was used to evaluate the temperature dependence of dynamic fracture toughness for two steels, pressure vessel steel A533B and high-carbon steel for tool SK4(JIS Standards). The obtained results for A533B steel was compared with those obtained by other workers.

EXPERIMENTAL

Loading device

The author previously developed a loading device to generate a well-controlled tensile stress wave incident to an edge crack in a long and wide strip specimen using a gas gun. A new device was constracted here for a narrow strip specimen. However, the basic mechanism is the same as tne previous one except that the coil spring force was used to accelerate a striker instead of tne gas gun. The device is schematically illustrated in Fig.1. The striker connected with the coil spring of which the other end was fixed to the frame was lifted to a certain height by the winch. It was accelerated downward by release of the energy stored in the spring when an electric magnet tied to the wire at the midway between the and striker tne winch, was switched off. When the striker struck the impact block, a tensile stress pulse was generated in the specimen, since the end of the specimen was quickly stretched and released soon. The tensile stress pulse propagated toward the other end of the specimen. The stress history in the specimen was calculated by means of the one-dimensional stress wave theory. The detail of the calculation was given in the previous paper(7). The stress pulse propagating in the specimen was measured by a semi-conductor strain gage mounted on the specimen surface at the distance of 400 mm from the free end of the specimen. Two kinds of the strikers were prepared. The one was 320 mm long and the other 160 mm. The former was used to generate a stress pulse with a 100 μs duration while the latter was for a stress pulse with a 50 μs duration.

Materials and specimen preparation

Materials used in this experiment were two kinds of steels, the pressure vessel steel A533B and high-carbon steel for tool SK4(JIS Standards). Their mechanical properties are shown in Table 1.

The specimen geometry used in the impact fracture toughness test was 32 mm wide, 6 mm thick and 1500 mm long as shown in Fig.2. The specimen consisted of three parts, which were 650 mm and 750 mm long mild steel plates, and 100 mm long testing steel plate having an edge crack at the mid section. These three plates were welded to make the 1500 mm long specimen. A fatigue crack was introduced from a saw cut in each specimen by cyclic loading. Total length of the crack and the saw cut was changed in the range between 0.47 and 0.66 in the ratio to the specimen width.

The cracked test section was soaked in liquid nitrogen or a mixture of etnyl-alcohol and dry-ice cubes to decrease the test temperature.

Critical amplitude stress pulse

An example of the stress histories measured by the strain gage s shown in Fig.3. It is seen that the first tensile stress pulse is the largest and it is quite sinusoidal rather than rectangular. Therefore, the first pulse is significant for crack initiation. The duration of the pulse was defined as the width at a half of the amplitude.

The amplitude of the first tensile stress pulse was increased with the height of the striker at the triggering. The experiment was begun at low neight of the striker so that the generated tensile pulse was not large enough to initiate the crack. Then, the height was increased little by little after each shot until the crack jump of 10 to 50 μm was detected at the specimen surface by the examination at 400-magnification with an optical microscope.

Critical amplitudes of the stress pulse for crack initiation determined by such a way are shown in Figs.4 and 5 as a function of the crack length at the room temperature. In the figures, solid marks indicate that no crack growth was observed; open marks indicate that crack growth was detected. Broken lines were drawn between the open and the solid marks to define the critical amplitude.

It is seen that the critical amplitude decreased with the increase of tne crack length and the pulse duration.

The critical amplitude of stress pulse for crack initiation was dependent on the test temperature as well as the crack length as shown in Figs.6 and 7. In the figures, the critical amplitude of 100 μs duration stress pulse for the fixed crack length is plotted against the test temperature. In the experimental range, it decreased monotonically for both steels as the temperature decreased .

DISCUSSION OF RESULTS

Crack tip stress intensity histories

As shown in Figs.4 and 5, the static fracture mechanics approach cannot be applied to the analysis of the results obtained here. Therefore, the dynamic stress analysis was carried out by means of the finite element code used in the previous work(7) for the specimen loaded by the critical amplitude stress pulse shown in Figs. 4 and 5. The specimen model used in the calculation is shown in Fig.8. The calculated stress intensity nistories for the crack lengths of a/w=0.47, 0.53 and 0.66 when a sinusoidal stress pulse was applied on the specimen are shown in Fig.9. Since the stress intensity is zero before the stress wave arrives at the crack, the time in the figure is measured from the moment when the stress wave reachs the crack

After the stress pulse struck the crack, the dynamic stress intensity increases with the time at the same rate independent of the crack length. However, since defracted wave by the crack was reflected at the specimen boundary to return the crack tip soon, the dynamic stress intensity histories for the different crack lengths began to deviate from each other. Those for the crack lengths of a/w=0.47, 0.53 and 0.66 were almost equal within 30 μs and seperated from each other beyond that time.

Dynamic fracture toughness at the room temperature

Some criteria of crack instability under stress wave loading have been proposed previously. The maximun dynamic stress intensity criterion(8) is the one that a crack immediately becomes unstable when the dynamic stress intensity exceeds the fracture toughness value of the material. The minimum time criterion(9) is the one that a crack starts to grow in an unstable manner when the dynamic stress intensity exceeds the fracture toughness value for a certain minimum time. When the increasing rate of the stress intensity is slow as shown in Fig.9, both criteria are almost identical. Therefore, the maximum stress intensity of which a crack experienced when it was loaded by the critical amplitude stress pulse for the crack initiation is shown as a function of the crack length in Figs.10 and 11. It is seen that the maximum stress intensity was independent of the crack length and the pulse duration. So, the value for each steel can be regarded as the dynamic fracture toughness K_{Id}.

The obtained toughness value were examined if they satisfied the ASTM E399 requirement for the plane strain condition(1). If we take the static value shown in Table 1 as the yield strength, the requirement was not satisfied for both steels. It is well known that some of the mechnical properties as well as the yield strength are sensitive against the loading rate. Since the yield strength of the both steels under the rapid loading were not measured in this experiment, they were estimated by the following formula given in the ASTM standards(10).

$$\sigma_{yD} = \sigma_{ys} + \frac{1198860}{T_x[\log_{10}(2\times10^7 t)]} - 187.4 \quad (MPa) \qquad (1)$$

where, σ_{ys} is static yield strength at the room temperature, Tx is the test temperature in K multiplied by a factor of 1.8 and t is the loading time in milliseconds.

For the 50 us duration pulse, the dynamic yield strengths of the A533B and the SK4 steel were computed as 712 and 547 MPa respectively. Even if these values are used, the specimen thickness enough to fulfil the ASTM requirement for the plane strain fracture toughness is 9 mm and 17.2 mm for the SK4 and the A533B steels respectively. Therfore, since the 6 mm thick specimens were used in this experiment, the obtained dynamic fracture toughnesses at the room temperature for the two steels were not regarded as those in the plane strain condition. However, macroscopic and microscopic observation results that shear lip width was very small, and that fracture mechanism was cleavage on the two steel specimens offer the negative against the above deduction. Then, the dynamic yield strength for the plane strain condition were inversely estimated by the ASTM requirement. Those should be greater than 1253 MPa and 765 MPa for the A533B and the SK4 steels respectively. The increase of the yield strength at very high loading rate to twice of the static value has been often observed for mild steel. Then, we cannot draw the conclusion that the results obtained in this experiment are not the plane strain fracture toughnesses for the two steels.

This will be discussed more later.

Dynamic fracture toughness under low temperature and its dependence on loading rate

The dynamic fracture toughness at the several test temperatures was computed from the results shown in Figs.6 and 7, and its dependence on the temperature is shown in Figs.12 and 13 for both steels.

In Fig.12, the dynamic fracture toughness of SK4 steel is compared with the fracture toughness measured under quasi-static loading within the limitation of the ASTM standards E399. The fracture toughness under the stress pulse loading decreased gently as the temperature decreased while that under the quasi-static loading decreased steeply.

In Fig.13, the results of A533B steel are compared with those under the slow loading rate and the rapid and quasi-static loading obtained by the other workers(11). It is noted that the fracture toughness is independent of the loading rate below -100°C and that the toughness under the slower loading rate is raised steeply from the lower emperature.

The steep increase in the fracture toughness under the quasi-static loading as shown in Figs.12 and 13 may result from change of the microscopic fracture mechanism. Fractographic observation with a transmit electron microscope indicated that ductile voids coalescing with the crack brought about the crack initiation in SK4 steel under the quasi-static loading at the room temperature while at the temperature of -85°C, cleavage fracture triggered the crack growth. Also, the fractographic observation indicated that under the stress pulse loading, the cleavage fracture caused the crack instability in both steels in the whole range of the temperature tested here.

Therefore, the fracture toughness at the high loading rate decreased gently as the temperature decreased, since the change in the fracture mechanism did not take place. It is very interesting to investigate what temperature brings about the transition from the ductile fracture mechanism to the brittle one in these steels under the stress pulse loading. However, it was not done in this work.

The loading rate dependence of the fracture toughness for A533B steel was previously investigated by the other workers(12) and is shown in Fig.14. It is seen in the figure that the loading rate dependence at the temperature of -47°C is negligible while the fracture toughness at the room temperature decreases as the loading rate increases.

The result obtained in this experiment is also plotted at $\dot{K}$ of 6.2×10^5MPa$\sqrt{m}$/s in the figure. This falls near the point where the lines for results at the temperatures of 24°C and -47°C intersect. This fact must suggest that the test method of dynamic fracture toughness is quite reasonable.

Crack tip plasticity under stress pulse loading

Fractographic works(13) indicated that the crack tip opening the crack tip blunting process can be related to the size of the stretched zone lying ahead of the initial crack tip on the fracture surface. If it is assumed that the crack tip is blunted to a semi-circle, the crack tip opening distance is equal to the stretched zone width multiplied by a factor of $\sqrt{2}$.

The stretched zone width was measured on the specimens where the crack instability had taken place and is shown in Fig.15 as a function of the temperature. The stretched zone width of SK4 steel was not so sensitive against the temperature as that of A533B steel. The dependence of the stretched zone width on the temperature for both steel is corresponding to that of the dynamic fracture toughness shown in Figs.12 and 13. The crack opening distance δ is given by the formula;

$$\delta = A\frac{K^2}{E\sigma_{ys}} \qquad (2)$$

where A is a constant and it is 0.44 for plane strain condition, K is stress intensity, E is Young's modulus and σ_{ys} is yield strength(14). Substitution of the dynamic fracture toughness and δ calculated from the critical stretched zone width shown in Fig.14 for K and δ in Eq.(2) gives the estimation of the yield strength of the material near the crack tip under the stress pulse loading. Those obtained were about 618 MPa and 687 MPa for A533B and SK4 respectively. They were about 1.2 times and twice larger than the static values.

It was tried to examine using these yield strengths whether the dynamic fracture toughness obtained in this experiment satisfied the ASTM E399 requirement of the plane strain condition. The requirement was filled for SK4 steel, but not for A533B. However, the observation of cleavage fracture at the initial crack tip in A533B steel specimen must suggest that the crack instability under the stress pulse loading took place in the plane strain condition.

SUMMARY

Cracks of several lengths in single-edge-notched strip specimens of A533B steel and SK4 steel were loaded by haversine-shaped tensile pulses of 50 μs and 100 μs duration under several temperatures below the room temperature. The critical amplitudes of the pulses for the crack instability were plotted as a function of crack length and it was indicated that the static fracture mechanics approach was invalid to analyse the results obtained here.

Dynamic stress intensity histories experienced by the cracks loaded by the critical amplitude stress pulses were computed using a dynamic finite element code. The computed results showed that the stress intensity histories for 50 μs and 100 μs duration stress pulses were not so short that the minimum time criterion for the dynamic crack instability should be used instead of the maximum stress intensity criterion to determine the dynamic fracture toughness of the two steels.

Dependence of the dynamic fracture toughness on the temperature was much moderate in comparison with that of the static toughness. This was interpretted by no change of the microscopic fracture mechanism, that was cleavage fracture in the two steels in the whole range of the test temperature.

Stretched zone width was measured for the specimens where the crack instability took place to investigate the crack tip plasticity under the stress pulse loading. The critical stretched zone width at the crack initiation decreased as the temperature decreased corresponding to the temperature dependence of the dynamic fracture toughness. Dynamic yield strength of the two steels was reasonably estimated from the relationship among the stress intensity, the yield strength and the crack opening displacement.

ACKNOWLEDGEMENT

The authers greatly appreciate useful discussion of the fractographic results given by Professor H. Kobayashi of Tokyo Institute of Technology.

USED SYMBOLS

a = crack length (m)
A = constant
δ = crack tip opening displacement (m)
K = stress intensity (MPa m)
$\dot{K}$ = increase rate of stress intensity (MPa$\sqrt{m}$/s)
K_{Id}= dynamic fracture toughness (MPa$\sqrt{m}$)
σ_{yD}= yield strength under dynamic loading (MPa)
σ_{ys}= yield strength under quasi-static loading (MPa)
t = time to fracture (ms)
Tx = temperature (K)
w = specimen width (m)

REFERENCES

1. 1983 Annual book of ASTM Standards, section 3-1, E399-83(1983) P.518
2. Server,W.L. and Tetelman,A.S., Engng.Frac.Mech 4(1972)367
3. Kalfhoff,J.F., Winkler,S., Bohme,W. and Klemn,W., Proc.5th Int. Conf.Fracture. 1981, Cannes, Vol.1, 363
4. Costin,L.S., Duffy,J, and Freund,L.B., ASTM STP 627(1977), 301
5. Homma,H and Gotoh,Y. To be published in Int.J.Fract
6. Kishida,K., and Nakagawa,K., J.Society of Mater. Science Japan 32-361(1983) 1096
7. Homma,H., Shockey,D.A. and Murayama,Y., J.Mech.Phys.Solids 31-3(1983),261
8. Achenbach,J.D. and Brock,L.M., Dynamic crack Propagation (edited by G.C. Sih)(1973),529 Noordhoff-Groningen, Leyden, Netherland
9. Kalthoff,J.F. and Shockey,D.A., J.apple.Phys. 48-3(1977),986
10. 1983 Annual book of ASTM Standards,section 3-1, E399-83, Special Requirements for Rapid-Load Plane-strain Fracture Toughness $K_{IC}(t)$ Testing(1983),549
11. Crosley,P.B. and Ripling,E.J., Nuclear Engng. and Design 17-1(1973),32
12. Shabbits,W.O., Trans. ASTM Ser.D, 87(1965), 257
13. Beachem,C.D., Fracture I. edited by H.Liebowitz Academic Press 1968,244
14. Rice,J.R., J.Mech.Phys.Solids,22(1974),17

Table 1 Mechnaical Properties of two steels

materials	yield strength MPa	ultimate strength MPa	elongation %
SK4	355	691	21.1
A533B	519	670	26.7

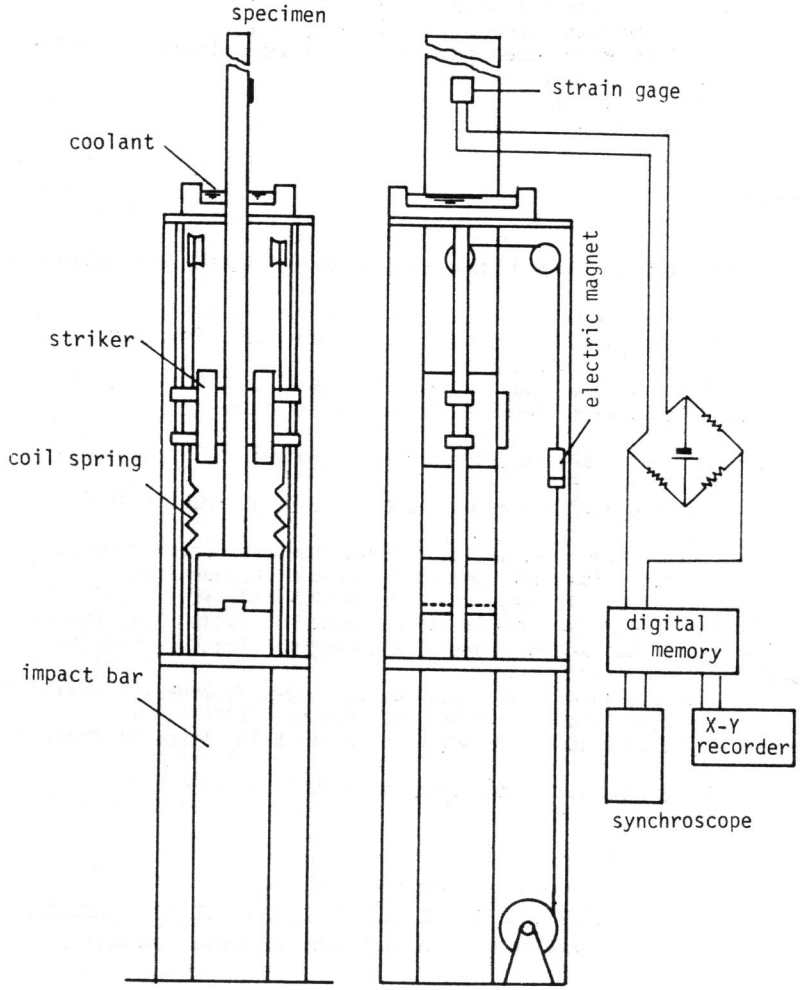

Fig.1 Loading device

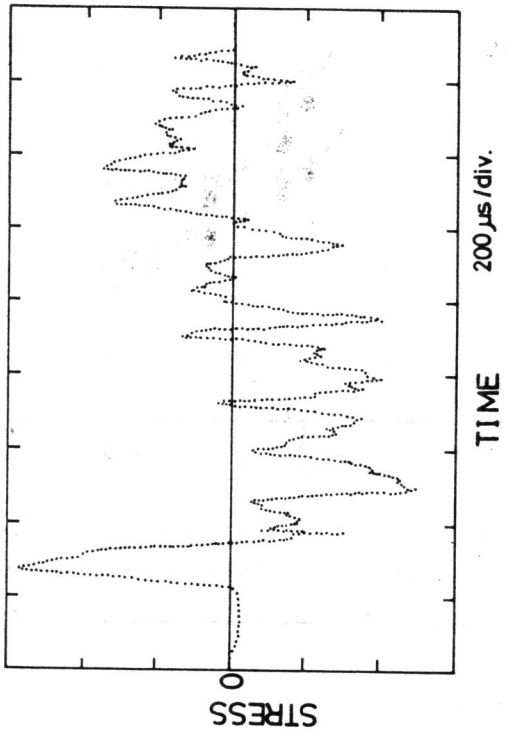

Fig.3 One of the measured stress histories in the specimen

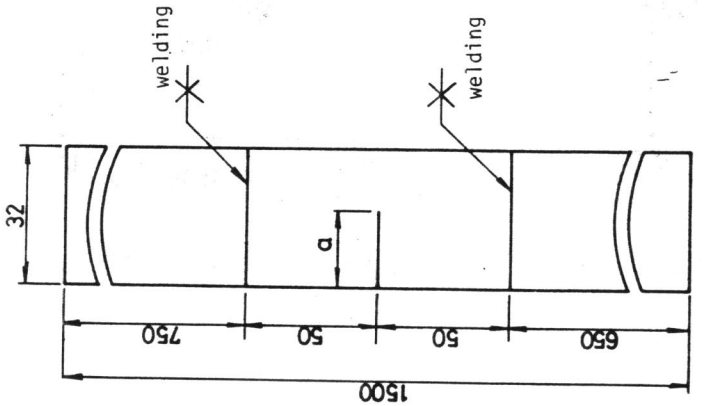

Fig.2 Specimen

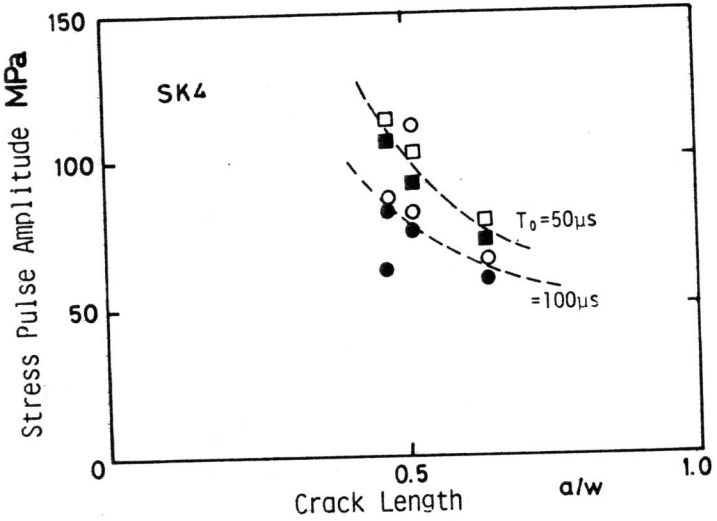

Fig.4 Critical stress pulse amplitude for crack initiation in SK4 (open marks indicate that the crack grew and solid ones, that the crack did not grow)

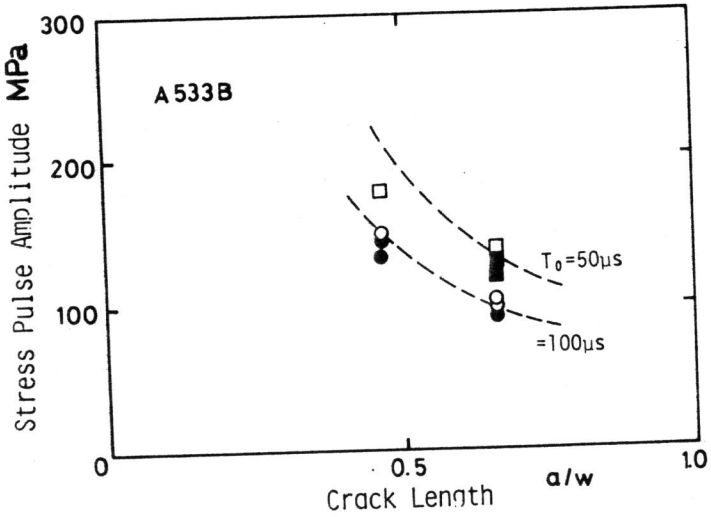

Fig.5 Critical stress amplitude for crack initiation in A533B (see Fig.4 for the marks)

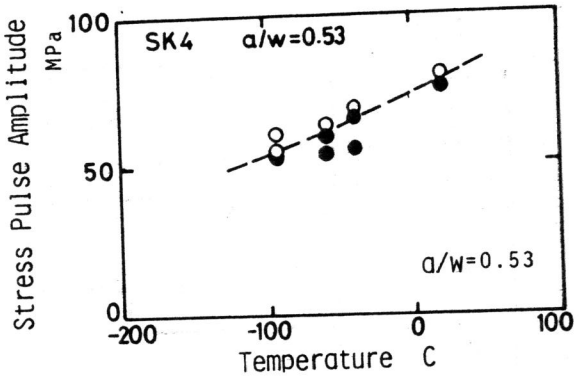

Fig.6 Critical stress pulse amplitude as a function of test temperature for SK4 under the pulse duration of 100 μs (see Fig.4 for the marks)

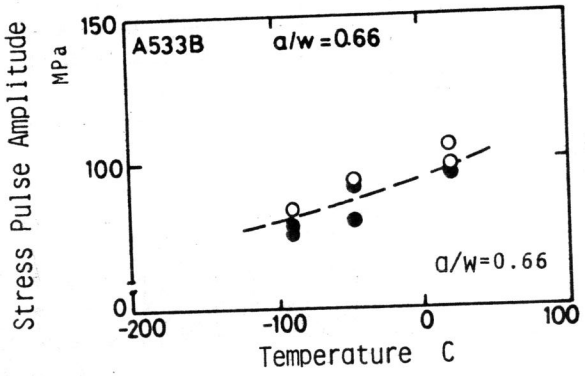

Fig.7 Critical stress pulse amplitude as a function of test temperature fro A533B under the pulse duration of 100μs (see Fig.4 for the marks)

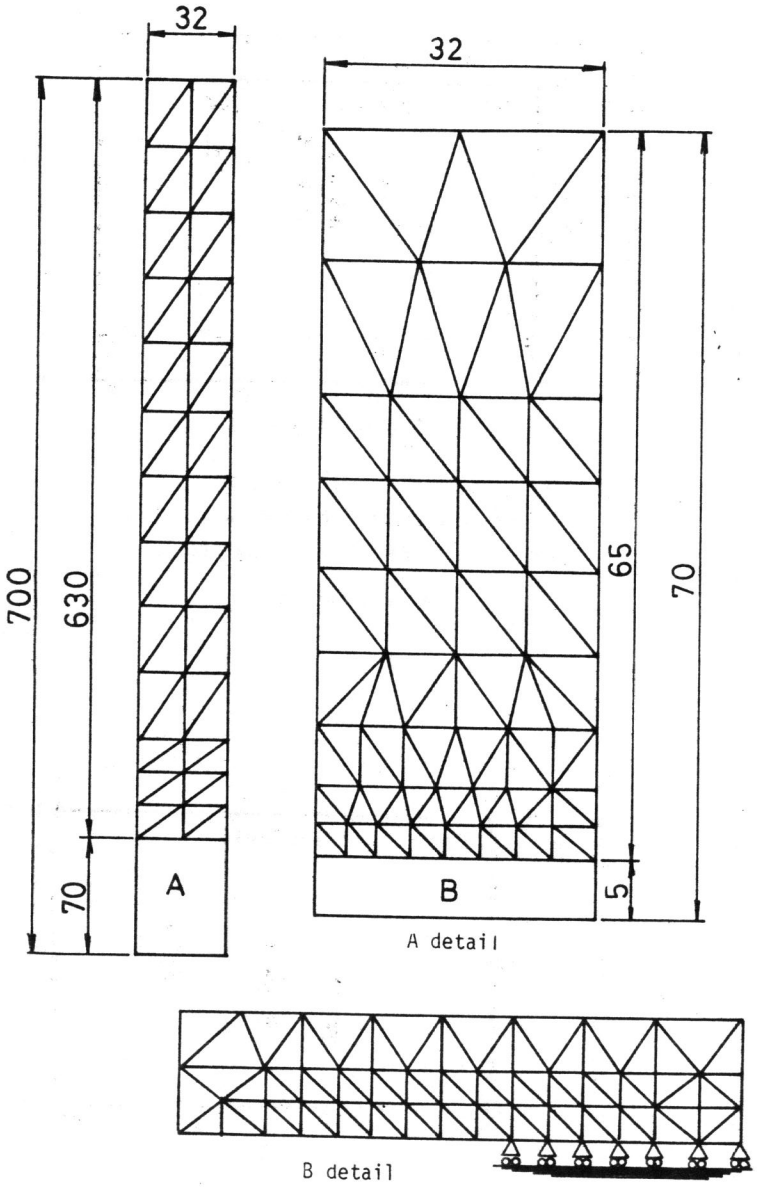

Fig.8 Mesh generation for FEM dynamic stress analysis

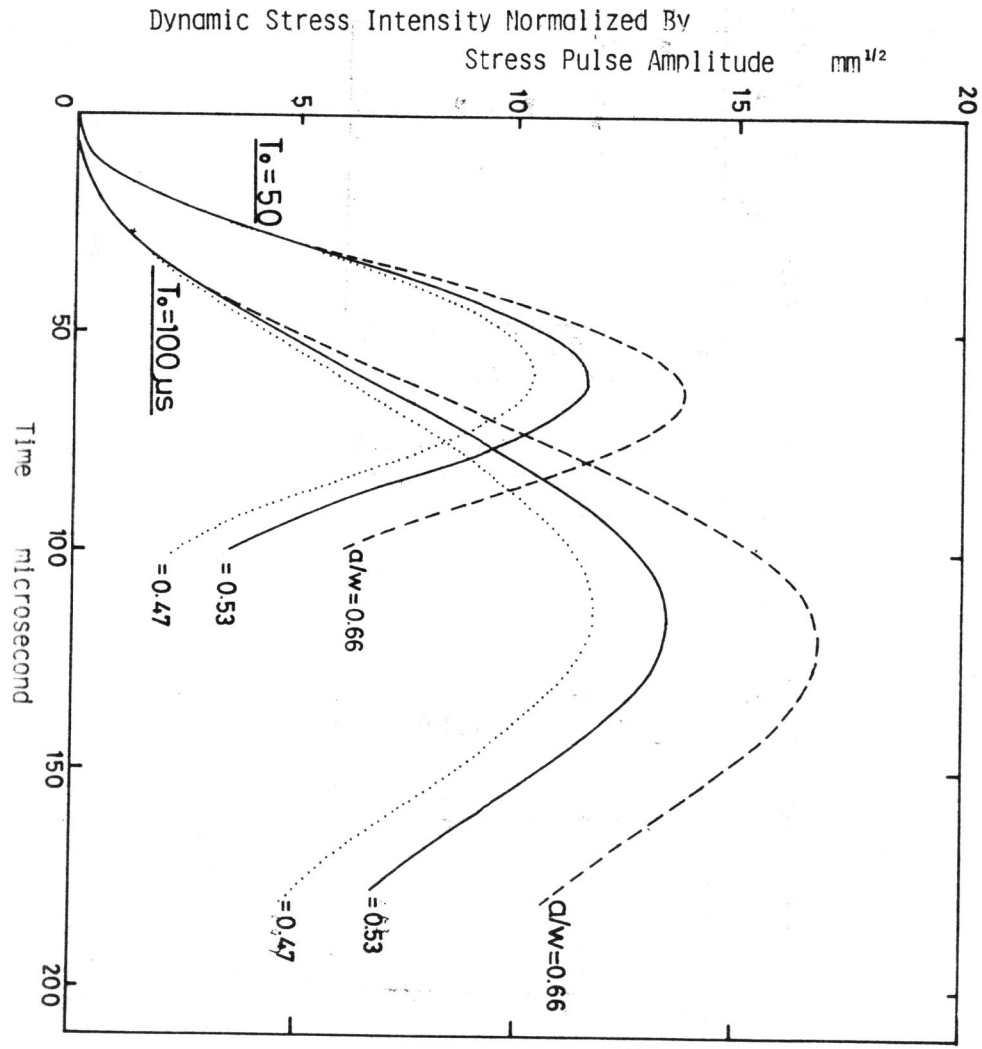

Fig.9 Dynamic stress intensity histories calculated by FEM for different crack lengths and pulse durations

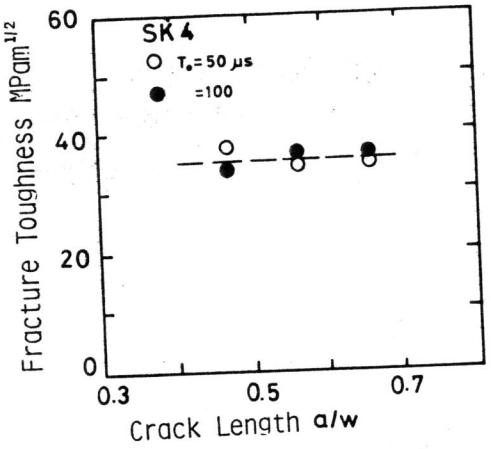

Fig.10 Critical dynamic stress intensity for crack initiation in SK4 as a function of the crack length

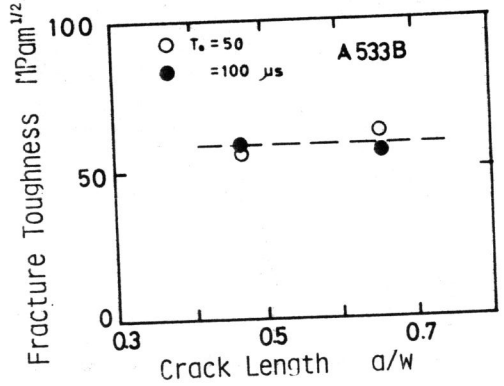

Fig.11 Critical dynamic stress intensity for crack initiation in A533B as a function of the crack length

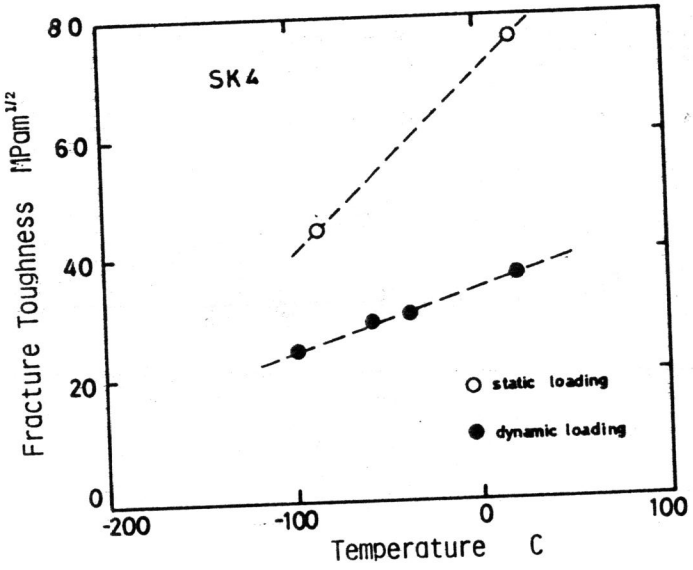

Fig.12 Temperature dependence of fracture toughness in SK4

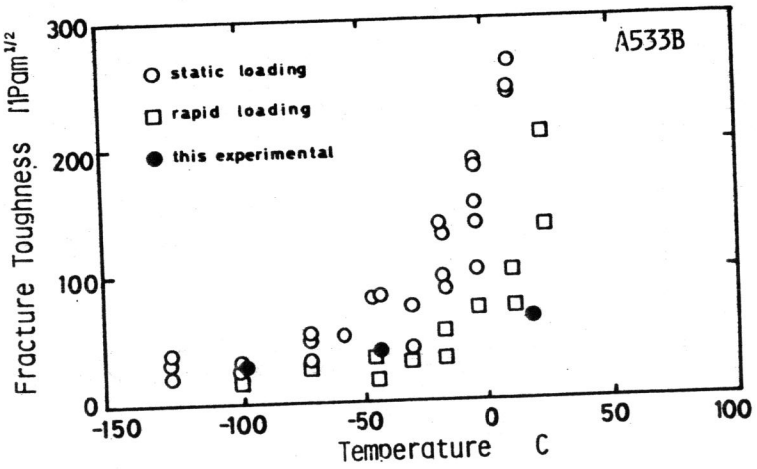

Fig.13 Temperature dependence of fracture toughness in A533B

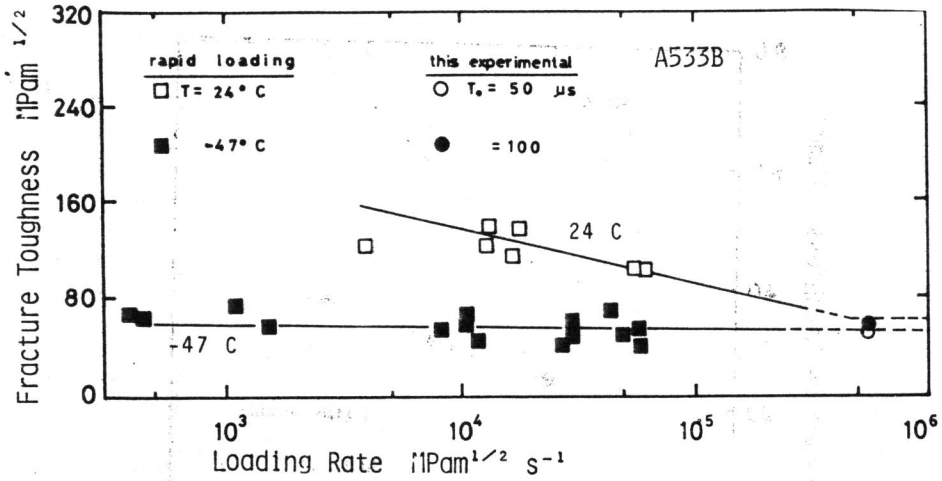

Fig.14 Fracture toughness of A533B as a function of loading rate

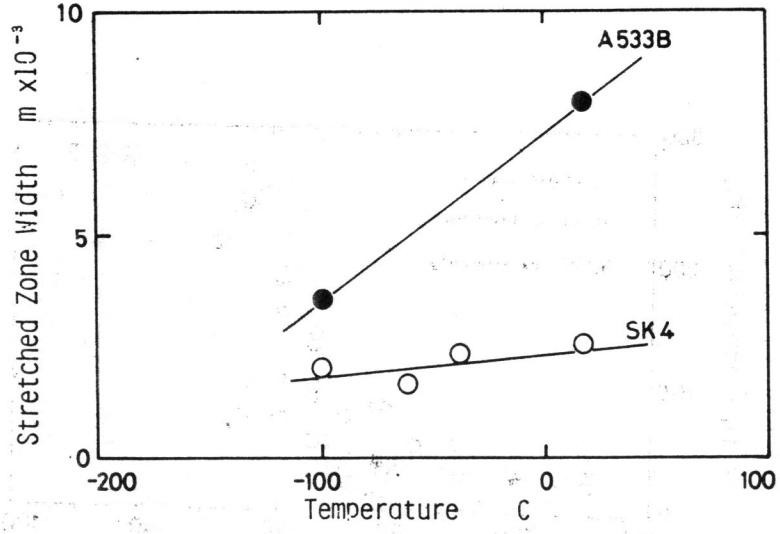

Fig.15 Stretched zone width on the surface fractured by stress pulse loading as a function of the test temperature